BEC BIOENERGETICS COMMUNICATIONS

Bioenerg Commun 2022.16
https://doi.org/10.26124/bec:2022-0016

Open Access

Experimental Communication and Review

Cite
Komlódi T, Tretter L (2022) The protonmotive force – not merely membrane potential. Bioenerg Commun 2022.16. https://doi.org/10.26124/bec:2022-0016

Author contributions
TK, LT wrote the manuscript.

Conflicts of interest
Authors declare no conflicts of interest.

Received 2022-04-06
Reviewed 2022-05-16
Resubmitted 2022-05-30
Accepted 2022-11-24
Published 2022-11-29

Open peer review:
Marcus Oliveira(editor)
Alicia Kowaltowski (reviewer)
Antonio Galina (reviewer)

Keywords
BCECF
intramitochondrial pH
matrix pH
ΔpH
mitochondria
mitochondrial membrane potential $\Delta\Psi_{mt}$
nigercin
protonmotive force *pmF*
reverse electron transfer RET
safranin
triphenylphosphonium TPP^+
valinomycin

The protonmotive force – not merely membrane potential

Timea Komlódi, László Tretter

Dept Biochem, Semmelweis Univ, Budapest, Hungary

Corresponding author:
komlodi.timea@med.semmelweis-univ.hu

Summary

The protonmotive force *pmF* establishes the link between electrical and chemical components of energy transformation and coupling of oxidative phosphorylation in the mitochondrial electron transfer system. The electric part corresponds to the mitochondrial membrane potential $\Delta\Psi_{mt}$ and the chemical part is related to the transmembrane pH difference ΔpH. Although the contribution of ΔpH to *pmF* is smaller than that of $\Delta\Psi_{mt}$, ΔpH plays an important role in mitochondrial transport processes and regulation of reactive oxygen species production. Measurement of both $\Delta\Psi_{mt}$ and ΔpH allows for calculation of *pmF*. Methods for monitoring $\Delta\Psi_{mt}$ such as fluorescence dyes are generally available, while determination of ΔpH is more challenging.

In this review, we focus on the application of the fluorescence ratiometric method using the acetoxymethyl ester form of 2,7-biscarboxyethyl-5(6)-carboxyfluorescein (BCECF/AM) for real-time monitoring of the intramitochondrial pH in isolated mitochondria. Knowing the intra- and extramitochondrial pH allows for calculating the ΔpH. Application of specific ionophores such as nigericin or valinomycin provides the possibility to dissect the two components of the *pmF*. We summarize the mitochondrial processes — such as production of reactive oxygen species — for which ΔpH plays an important role.

1. Protonmotive force

The chemiosmotic theory on protonmotive force *pmF* (Δp, or $\Delta_m F_{H+}$) was postulated by Peter Mitchell in 1961 with four theorems describing the coupling of ATP synthesis to the electrochemical potential difference across the mitochondrial inner membrane mtIM (Gnaiger 2020; Mitchell 1961, 1967; Mitchell, Moyle 1968). The oxidation of respiratory fuel substrates by electron transfer to O_2 is accompanied by H^+ translocation through respiratory Complexes I, III and IV from the matrix to the intermembrane space. This process results in a negatively charged matrix and positively charged intermembrane space. The proton and charge concentration difference create an electrochemical potential difference called *pmF*. The *pmF* generated by proton pumps of the electron transfer system ETS, is utilized to drive the synthesis of ATP. The *pmF* has a chemical part $\Delta_d F_{H+}$ related to ΔpH and an electric component $\Delta_{el} F_{p+}$ corresponding to the mitochondrial membrane potential $\Delta\Psi_{mt}$ (Gnaiger 2020),

$$\Delta_m F_{H+} = \Delta_d F_{H^+} + \Delta_{el} F_{p^+}$$

$\Delta_d F_{H^+}$ is specific for hydrogen ions H^+ and represents the chemical partial force of diffusion independent of charge. $\Delta_{el} F_{p^+}$ is the electric partial force related to the charge distribution of protons p^+ irrespective of the nature of the ions involved. The net distribution of ions (not only H^+) generates an internal electrical field across the two sides of mtIM. The cations are driven to move according to the electrical potential, from the positive side of the membrane to the negative side and the anions in the opposite direction.

The components of the *pmF* can be measured separately. Methods for monitoring $\Delta\Psi_{mt}$ are generally available, whereas determination of ΔpH is more challenging. In many studies, the contribution of ΔpH to *pmF* is ignored, reporting only $\Delta\Psi_{mt}$ values even in cases when a conversion from ΔpH to $\Delta\Psi_{mt}$ is not proven. A shift between the two components can occur in the presence of specific ionophores (Komlódi et al 2018).

1.1. Mitochondrial membrane potential

Lipophilic cationic fluorescence probes and ion-selective electrodes are most frequently used to measure changes of $\Delta\Psi_{mt}$ in real-time. Lipophilic cationic fluorescent probes such as safranin are able to enter the negatively charged mitochondrial matrix, bind to anionic sides and create dimers or oligomers, causing fluorescence quenching and thereby to a decrease of the fluorescence signal (Akerman, Wikström 1976; Figueira et al 2012; Kauppinen, Hassinen 1984; Krumschnabel et al 2014). In the LEAK state, when $\Delta\Psi_{mt}$ is highest (~170 mV), safranin accumulates in the mitochondrial matrix which is reflected by the decrease of the fluorescence signal (Figure 1A). If $\Delta\Psi_{mt}$ is lower — e.g. in the presence of ADP in the OXPHOS state $\Delta\Psi_{mt}$ decreases by ~25 mV (Chinopoulos et al 2010) — the safranin concentration is higher in the extramitochondrial compartment which is shown by the increase of the fluorescence signal. Upon addition of an uncoupler (protonophore) $\Delta\Psi_{mt}$ further decreases. Mitochondrial protein and dye concentration affect the fluorescence intensity (Scaduto Jr, Gotyohann 1999). A linear relationship between fluorescence intensity and $\Delta\Psi_{mt}$ can be observed only within limited concentration ranges and ratios of safranin and mitochondria due to fluorescence quenching (Figueira et al 2012). Additionally, fluorescence quenching could affect the $\Delta\Psi_{mt}$ calculated from the logarithmic Nernst equation which is used to describe the distribution of the fluorescence dyes in the mitochondria (Scaduto Jr, Gotyohann 1999). Calibration of the fluorescence signal of safranin can be carried out with KCl titration in

the presence of valinomycin as discussed in detail by Figueira et al 2012. Of note, owing to the complexity of the fluorometric measurement and calibration, we have used TPP^+ to calculate $\Delta\Psi_{mt}$ expressed in mV (Komlódi et al 2018; Tretter et al 2007).

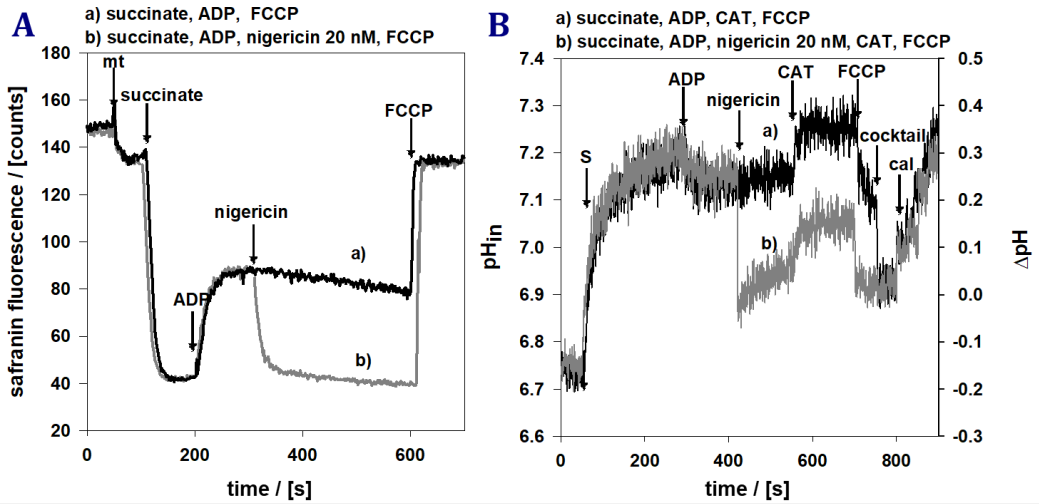

Figure 1. Mitochondrial membrane potential (A), and intramitochondrial pH pH_{in} and transmembrane ΔpH (B). Mitochondria isolated from guinea pig brain. mt-Membrane potential $\Delta\Psi_{mt}$ was measured by safranin fluorescence, pH_{in} was monitored by BCECF, and ΔpH was calculated as described (Komlódi et al 2018). Addition of succinate (5 mM) led to hyperpolarization of $\Delta\Psi_{mt}$ and increase of pH_{in}; ADP (2 mM) partially depolarized $\Delta\Psi_{mt}$ and decreased pH_{in} and ΔpH; nigericin (20 nM) increased $\Delta\Psi_{mt}$ and decreased ΔpH; carboxyatractyloside CAT (2 μM; inhibitor of the adenine nucleotide translocase) increased pH_{in} owing to H^+ accumulation in the intermembrane space; carbonyl cyanide-p-trifluoromethoxyphenylhydrazone FCCP (250 nM; uncoupler) decreased ΔpH, therefore depolarized $\Delta\Psi_{mt}$ and decreased pH_{in}. A mixture of ionophores (8 μM nigericin; 2.5 μM gramicidin; 8 μM monensin) was added to equalize pH_{in} and extramitochondrial pH pH_{ex}. The BCECF fluorescence was calibrated by KOH. The measurements were carried out in standard medium A.

Alternatively, $\Delta\Psi_{mt}$ can be estimated based on the distribution of a lipophilic cation such as tetraphenylphosphonium ion TPP^+ detected by an ion-selective electrode (Kamo et al 1979; Komlódi et al 2018; Rottenberg 1984). The accumulation of TPP^+ in the mitochondria is described by the mitochondrial uptake and binding to the mtIM (and mtOM) is known as 'unspecific binding', which may occur independent of the membrane potential, and hence is not based on the Nernst equation and requires corrections. The advantage of this method is that the absolute $\Delta\Psi_{mt}$ expressed in mV can be determined. Upon hyperpolarization of $\Delta\Psi_{mt}$, TPP^+ accumulates in the matrix leading to a decrease of the extramitochondrial TPP^+ concentration (more accurately: TPP^+ activity) accessible to the ion-selective electrode. Noteworthy, TPP^+ is more sensitive in the range of high $\Delta\Psi_{mt}$ values than safranin (Starkov, Fiskum 2003).

1.2. ΔpH

Although the contribution of ΔpH to *pmF* is smaller than that of $\Delta\Psi_{mt}$, ΔpH plays an important role in mitochondrial transport processes such as transport of inorganic phosphate (Hoek et al 1970) or calcium influx (Bernardi, Azzone 1979).

Fluorescent indicators such as the acetoxymethyl ester form of 2,7-biscarboxyethyl-5(6)-carboxyfluorescein BCECF/AM (Jung et al 1989; Komlódi et al 2018) are widely used to measure pH_{in}. Mitochondria are first loaded with the membrane-permeable esterified form of the indicator, which is then hydrolyzed by intramitochondrial esterases to non-permeable, free fluorophores, whose fluorescence depends on their protonation/deprotonation (Zółkiewska et al 1993). BCECF has the advantage of having pH-dependent and pH-independent regions in its excitation spectrum, therefore, its fluorescence can be monitored at two excitation wavelengths allowing for ratiometric fluorescence measurement (Han, Burgess 2010; Komlódi et al 2018). These data are correlated to pH values after equalizing intramitochondrial pH (pH_{in}) and extramitochondrial pH (pH_{ex}) using a mixture of ionophores as previously described (Komlódi et al 2018; Tretter et al 2007).

In isolated mammalian mitochondria, *in vitro* ΔpH depends on the composition of the respiration medium, substrates (pathway control state) and respiratory coupling control states. Addition of respiratory substrates e.g. succinate leads to alkalization of pH_{in} in the LEAK state (without ADP) owing to H^+ efflux from the mitochondrial matrix via respiratory Complexes (Figure 1). Addition of ADP decreases pH_{in} due to H^+ influx into the mitochondrial matrix via the proton channel of the F_1F_0-ATPase. Uncouplers further decrease pH_{in}, ΔpH and $\Delta\Psi_{mt}$ due to H^+ translocation to the matrix. In a medium containing saccharose and low [K^+] (4 mM), the ΔpH is ~ 0.6-0.8, whereas at high K^+ concentration (~120 mM) ΔpH is 02.-0.3 in the presence of 2 mM phosphate (Komlódi et al 2018; Mitchell, Moyle 1968). Vajda et al (2009) reported a ΔpH lower than 0.15 in a buffer with 120 mM KCl with 10 mM inorganic phosphate P_i. P_i plays an important role in regulation of matrix pH. P_i enters the mitochondrial matrix via the P_i/OH^- exchanger or via co-transport with H^+ resulting in acidification of the matrix and decrease of ΔpH. A decrease of ROS generation is attributed to a decrease of pH_{in}, whereas alkalization is ascribed to elevated ROS release (Komlódi et al 2018; Selivanov et al 2008). In succinate-energized guinea pig brain mitochondria in the LEAK state the ΔpH was higher in the absence than in the presence of P_i (data not shown). Importantly, BCECF fluorescence can be easily calibrated after dissipation of ΔpH using ionophores followed by adding KOH solutions and measuring BCECF fluorescence and pH of the solution with a glass electrode, when the pH_{in} and pH_{ex} are equal as a consequence of ionophore action (Komlódi et al 2018; Tretter et al 2007).

1.3. Ionophores

Ionophores are widely used compounds when studying $\Delta\Psi_{mt}$ or ΔpH in isolated mitochondria. Valinomycin is a K^+ ionophore and its effect depends on its concentration and the K^+ concentration (Bernardi 1999; Komlódi et al 2018; Ligeti, Fonyó 1977). Valinomycin added in the nM range, in the presence of low K^+ concentration (~ 4 mM) increases pH_{in} which is explained by H^+ efflux and P_i/OH^- exchange leading to depolarization of $\Delta\Psi_{mt}$ and increase of mitochondrial respiration. Nigericin is an electroneutral K^+/H^+ antiporter which is widely used to shift ΔpH further to $\Delta\Psi_{mt}$ by a decrease of pH_{in} and compensatory increase of $\Delta\Psi_{mt}$ (Bernardi 1999; Henderson et al 1969; Garlid, Paucek 2001; Komlódi et al 2018; Lambert, Brand 2004; Selivanov et al 2008). It is, however, important to note that nigericin added at the lowest possible concentration which caused the maximal hyperpolarization of $\Delta\Psi_{mt}$ in guinea pig brain mitochondria does not fully dissipate ΔpH leading to a decrease of P_i flux and of P_i concentration in the matrix, but it establishes a new equilibrium at a lower pH_{in} in the

presence of high [K^+] (Komlódi et al 2018). Decrease of [P_i] in the matrix reduces F_1F_0-ATPase activity resulting in decrease of mitochondrial respiration in isolated mitochondria (Metelkin et al 2009).

2. Role of ΔpH in reactive oxygen species generation

It is well known that production of reactive oxygen species (ROS) by mitochondria is sensitive to changes of the *pmF* components (Komlódi et al 2018; Lambert, Brand 2004; Selivanov et al 2008). In murine mitochondria, succinate-evoked reverse electron transfer (RET) in the LEAK state promotes the highest rate of ROS production which is sensitive to changes of the *pmF* components (Votyakova, Reynolds 2008; Zoccarato et al 2011). It is generally accepted that decrease of the $\Delta\Psi_{mt}$ leads to a decrease in RET-evoked ROS formation supported by succinate (Korshunov et al 1997; Komlódi et al 2018; Lambert, Brand 2004; Selivanov et al 2008; Votyakova, Reynolds 2001), whereas hyperpolarization of $\Delta\Psi_{mt}$ induces ROS production. Increase of the absolute pH rises succinate-supported ROS generation in the LEAK state due to the stabilization of semiquinone radicals (Komlódi et al 2018; Selivanov et al 2008). It is difficult to evaluate the direct effect of ΔpH on ROS production, because ΔpH usually changes in the same direction as $\Delta\Psi_{mt}$. For example, uncouplers cycling across the mtIM with protons decrease both the $\Delta\Psi_{mt}$ and the ΔpH which leads to increase of respiration and decrease of ROS production. However, it is hard to evaluate whether the reduction in ROS production are caused by changes in $\Delta\Psi_{mt}$ or ΔpH. To determine which component of the *pmF* plays a greater role in regulation of RET, ionophores such as nigericin (K^+/H^+ antiporter) and valinomycin (K^+ ionophore) can be used to dissect the components of the *pmF*. There is no general agreement on how these ionophores influence the RET-induced ROS generation. Nigericin hyperpolarizes $\Delta\Psi_{mt}$, decreases ΔpH and moderately increases RET-driven ROS formation using succinate in brain and heart mitochondria isolated from guinea pigs (Komlódi et al 2018). In contrast, valinomycin depolarizes $\Delta\Psi_{mt}$, increases ΔpH and decreases the rate of ROS production using succinate as CHNO-fuel substrate. Based on these results it can be concluded that $\Delta\Psi_{mt}$ is the dominant component of the *pmF* over ΔpH in modulation of succinate- or α-glycerophosphate-induced ROS formation in the LEAK state in guinea-pig brain mitochondria (Komlódi et al 2018). Lambert and Brand (2004), however, described that succinate-evoked RET depends more on ΔpH than $\Delta\Psi_{mt}$ using nigericin, whereas Selivanov et al (2008) reported that the acute pH rather than ΔpH is dominant over $\Delta\Psi_{mt}$ in regulation of RET. Although the literature is controversial on which component of *pmF* plays a greater role in regulation of RET, it is obvious that the contribution of ΔpH to *pmF* is not negligible.

3. Role of ΔpH and matrix pH in the reversal of F_1F_0-ATPase

The mitochondrial F_1F_0-ATPase is able to synthesize and hydrolize ATP (Boyer 2002; Rouslin et al 1986; Walker 1994). F_1F_0-ATPase uses the *pmF* to generate ATP, thus, its reversal also depends on the *pmF*. Since ΔpH is the smaller component of the *pmF*, the reversal of F_1F_0-ATPase mostly depends on $\Delta\Psi_{mt}$. The $\Delta\Psi_{mt}$ values at which the F_1F_0-ATPase starts hydrolyzing ATP, which is called reversal potential, controlled mainly by the ADP/ATP ratio in the matrix, phosphate concentration, and H^+/ATP coupling ratio (Chinopoulos et al 2010 and 2011). Decrease of $\Delta\Psi_{mt}$, e.g. owing to inhibition of the ETS, results in the reversal of F_1F_0-ATPase allowing hydrolysis of mitochondrial ATP

generated via substrate-level phosphorylation catalyzed by succinate-CoA ligase to maintain $\Delta\Psi_{mt}$ (Chinopoulos et al 2010; 2011; Kiss et al 2014; Komlódi et al 2018; Lambeth et al 2004). Under this condition F_1F_O-ATPase operates in the reverse mode, whereas adenine nucleotide translocase ANT operates in the forward mode. This has paramount importance under pathological conditions, because in a specific $\Delta\Psi_{mt}$ range mitochondria can avoid using cytosolic ATP to maintain $\Delta\Psi_{mt}$, thus showing better survival rate for the cells. However, further decline of $\Delta\Psi_{mt}$ — despite of the ATP hydrolysis — leads to reversal of the ANT (Metelkin et al 2009), thus, transporting cytosolic ATP into the mitochondria (Chinopoulos et al 2010). ANT has its own reversal potential which is controlled by the participating components such as the ADP/ATP ratio in the matrix and cytosol (Chinopoulos et al 2010).

Although ΔpH is the smaller component of the *pmF*, the question arises how it affects the reversal potential of the F_1F_O-ATPase and ANT. Chinopoulos (2011) reported computer simulations in which ΔpH was kept constant and the reversal potentials of F_1F_O-ATPase and ANT were lower. When pH_{in} and thus ΔpH was decreased, the reversal potentials were shifted to the polarizing potentials. Importantly, the reversal potential of F_1F_O-ATPase was more affected by decline of pH_{in} than that of ANT.

Individual cristae within a mitochondrion can have different local $\Delta\Psi_{mt}$ thus depolarization might affect some cristae but not others (Wolf at el 2019). In line with this, Rieger et al (2014) observed that ΔpH exists between respiratory Complexes and the F_1F_O-ATPase leading to built-up of intracristal local *pmF*. Since the local *pmF* around the F_1F_O-ATPase is low during OXPHOS (Rieger et al 2021), the inhibitory factor 1, which is an endogenous regulator of F_1F_O-ATPase responsible for its dimerization (Campanella et al 2009), is required to block reversal of the F_1F_O-ATPase (Rieger et al 2021).

4. Materials and methods

4.1. Mitochondrial isolation

Animal experiments were carried out in accordance with the International Guiding Principles for Biomedical Research Involving Animals and Guidelines for Animal Experiment at Semmelweis University after decapitation of albino guinea pigs. According to the EU Directive " Directive 2010/63/eu of the European Parliament and of the Council of 22 September 2010 on the protection of animals used for scientific purposes" (Chapter 1, Article 3, Definitions 1, Paragraph 2: "killing the animals solely for the use of their organs or tissues"), the applied procedure above does not require any further specific permission.

The mitochondrial protein content was determined with the modified biuret according to Bradford (Bradford 1976).

After decapitation the brain cortex was removed and placed in ice-cold buffer A (in mM: 225 mannitol, 75 sucrose, 5 HEPES, 1 EGTA), pH=7.4, as described previously (Rosenthal et al 1987; Komlódi 2018). The brain was washed in buffer A and cut into small pieces followed by homogenization with a Potter-Elvehjem homogenizer. The homogenate was centrifuged for 3 min at 1300 *g* and then the supernatant was recentrifuged for 10 min at 20 000 *g*. The pellet was suspended in 15 % Percoll and layered on a discontinuous Percoll gradient with 40 % below and 23 % in the middle, which was centrifuged for 8 min at 30 700 *g* without brakes. The lower mitochondrial

fraction was resuspended in buffer A and centrifuged at 16 600 *g* for 10 min. The supernatant was discharged, and the pellet was resuspended in buffer A and centrifuged at 6300 *g* for 10 min. The supernatant was removed and the pellet was resuspended in buffer B (in mM: 225 mannitol, 75 sucrose, 5 HEPES), pH =7.4.

The heart was washed in the homogenization buffer (in mM: 200 mannitol, 50 sucrose, 5 NaCl, 5 MOPS, 1 EGTA) and 0.1 % BSA, pH 7.15, and cut into small pieces in 2.5 mL homogenization buffer supplemented with 10 U protease (protease from Bacillus licheniformis; Type VIII). Then, the heart was homogenized in 17.5 mL homogenization buffer and the suspension was centrifuged for 10 min at 10 500 *g*. The supernatant was removed, and the pellet was resuspended in 25 mL homogenization buffer and centrifuged for 10 min at 3000 *g*. Finally, the supernatant was centrifuged for 10 min at 10 500 *g* and the remaining pellet was suspended in the homogenization buffer.

4.2. Mitochondrial H_2O_2 production

H_2O_2 production was measured with Amplex UltraRed (AmR) in combination with horseradish peroxidase (HRP) in isolated mitochondria (protein concentration 0.05 mg/mL). AmR (3 μM) is oxidized by H_2O_2 in a reaction catalyzed by HRP (5 U/ 2 mL) forming a red fluorescent dye, Amplex UltroxRed (ex. 550 nm; em. 585 nm). Measurements were carried out at 37 ˚C using PTI Deltascan fluorimeter (Photon Technology International; Lawrenceville, NJ). Fluorescence signal was calibrated with 5 nM H_2O_2 at the end of each experiment.

4.3. Mitochondrial membrane potential using TPP^+

$\Delta\Psi_{mt}$ was estimated by the distribution of the tetraphenylphosphonium ion (TPP^+) using a custom-made TPP^+-selective electrode in the standard medium (Kamo et al 1979), as described previously (Komlódi et al 2018). $\Delta\Psi_{mt}$ was calculated using the Nernst equation and the reported binding correction factor for brain mitochondria (Rottenberg 1984; Rolfe et al. 1994). The calculation was performed according to Rottenberg (1984) assuming that the mitochondrial matrix volume is 1 μL/mg protein (Chalmers, Nicholls 2003).

4.4. Intramitochondrial pH (pH_{in})

pH_{in} of isolated mitochondria was measured as described previously (Komlódi et al 2018). Briefly, 100 uL mitochondria (ca. 35-40 mg/mL protein) were loaded with acetoxymethyl ester of BCECF (50 μM) present in buffer B (in mM: 225 mannitol, 75 sucrose, 5 HEPES, 0.1 EGTA), pH 7.4, supplemented with 0.1 mM ADP for 10 min at 25 ˚C. Then, 325 μL ice-cold buffer B with 0.1 mM ADP was added. Loaded mitochondria were centrifuged for 2 min at 13 000 *g*. The pellet was resuspended in 450 uL buffer B and centrifuged again for 2 min at 13 000 *g*. Then, the pellet was suspended in 450 μL buffer B without ADP and left for 15 min, followed by centrifugation for 2 min at 13 000 *g*. Afterwards, the supernatant was discarded and the pellet was supplemented with 13 μL buffer B, kept on ice. BCECF-loaded mitochondria were used within 90 min. For measuring fluorescence, 3 μL aliquots of mitochondria were diluted in 2 mL of standard medium A or B. Fluorescence ratios were determined with Photon Technology International (PTI; Lawrenceville, NJ) Deltascan fluorescence spectrophotometer using 440 nm and 505 nm excitation and 540 nm emission wavelengths. Leakage of BCECF from

mitochondria was determined by centrifugation of loaded mitochondria and measuring the fluorescence of the supernatant. Corrections were made by subtracting the fluorescence values measured in the supernatant remaining after leakage of BCECF from the experimental values. For calibration, the external and internal pH were equilibrated by addition of 8 mM nigericin (K^+/H^+ antiporter), 2.5 mM gramicidin (Na^+/K^+ ionophore), and 8 mM monensin (Na^+/H^+ antiporter).

4.5. Chemicals and media

Standard laboratory reagents except for ADP were obtained from Sigma (St. Louis, MO). ADP was purchased from Merck Group (Darmstadt, Germany). BCECF/AM and Amplex UltraRed were obtained from Molecular Probes.

Experiments using nigericin were carried out in standard medium A (in mM): 125 KCl, 20 HEPES, 2 KH_2PO_4, 0.1 EGTA, 1 $MgCl_2$, and 0.025 % BSA. Experiments with valinomycin were performed in standard medium B (in mM): 240 sacharose, 10 Tris, 2 KH_2PO_4, 4 KCl, 0.1 EGTA, 1 $MgCl_2$, and 0.025 % BSA.

Acknowledgements

This project was supported by the Hungarian Brain Research Program 2 (2017-1.2.1-NKP-2017-00002 to Vera Adam-Vizi, Semmelweis University), STIA-OTKA-2021 grant (from the Semmelweis University, to A.A.) and TKP2021-EGA-25 grant to A.A. Project no. TKP2021-EGA-25 has been implemented with the support provided by the Ministry of Innovation and Technology of Hungary from the National Research, Development and Innovation Fund, financed under the TKP2021-EGA funding scheme.

Abbreviations

$\Delta\Psi_{mt}$	mitochondrial membrane potential	mtIM	mitochondrial inner membrane
ΔpH	transmembrane pH	mtOM	mitochondrial outer membrane
ANT	adenine nucleotide translocase	pH_{ex}	extramitochondrial pH
BCECF/AM	AM acetoxymethyl ester form of 2,7-biscarboxyethyl-5(6)-carboxyfluorescein	pH_{in}	intramitochondrial pH
		pmF	protonmotive force
FCCP	carbonyl cyanide-p-trifluoromethoxyphenylhydrazone	RET	reverse electron transfer
		ROS	reactive oxygen species
IF1	inhibitory factor 1	TPP^+	tetraphenylphosphonium

References

Akerman KEO, Wikström MKF (1976) Safranine as a probe of the mitochondrial membrane potential. https://doi.org/10.1016/0014-5793(76)80434-6

Bernardi P (1999) Mitochondrial transport of cations: channels, exchangers, and permeability transition. https://doi.org/10.1152/physrev.1999.79.4.1127

Bernardi P, Azzone GF (1979) delta pH induced calcium fluxes in rat liver mitochondria. https://doi.org/10.1111/j.1432-1033.1979.tb04272.x

Boyer PD (2002) A research journey with ATP synthase. https://doi.org/10.1074/jbc.x200001200

Bradford MM (1976) A rapid and sensitive method for the quantitation of microgram quantities of protein utilizing the principle of protein-dye binding. https://doi.org/10.1006/abio.1976.9999

Campanella M, Parker N, Choon Hong Tan, Hall AM, Duchen MR (2009) IF(1): setting the pace of the F(1)F(o)-ATP synthase. https://doi.org/10.1016/j.tibs.2009.03.006

Chalmers S, Nicholls DG (2003) The relationship between free and total calcium concentrations in the matrix of liver and brain mitochondria. https://doi.org/10.1074/jbc.M212661200

Chinopoulos C (2011) The "B space" of mitochondrial phosphorylation. https://doi.org/10.1002/jnr.22659

Chinopoulos C, Gerencser AA, Mandi M, Mathe K, Töröcsik B, Doczi J, Turiak L, Kiss G, Konràd C, Vajda S, Vereczki V, Oh RJ, Adam-Vizi V (2010) Forward operation of adenine nucleotide translocase during F0F1-ATPase reversal: critical role of matrix substrate-level phosphorylation. https://doi.org/10.1096/fj.09-149898

Figueira TR, Melo DR, Vercesi AE, Castilho RF (2012) Safranine as a fluorescent probe for the evaluation of mitochondrial membrane potential in isolated organelles and permeabilized cells. https://doi.org/10.1007/978-1-61779-382-0_7

Garlid KD, Paucek P (2001) The mitochondrial potassium cycle. https://doi.org/10.1080/15216540152845948

Gnaiger E (2020) Mitochondrial pathways and respiratory control. An introduction to OXPHOS analysis. 5th ed. https://doi.org/10.26124/bec:2020-0002

Han J, Burgess K (2010) Fluorescent indicators for intracellular pH. https://doi.org/10.1021/cr900249z

Henderson PJ, McGivan JD, Chappell JB (1969) The action of certain antibiotics on mitochondrial, erythrocyte and artificial phospholipid membranes. The role of induced proton permeability. https://doi.org/10.1042/bj1110521

Hoek JB, Lofrumento NE, Meyer AJ, Tager JM (1970) Phosphate transport in rat-liver mitochondria. https://doi.org/10.1016/0005-2728(71)90096-X

Jung DW, Davis MH, Brierley GP (1989) Estimation of matrix pH in isolated heart mitochondria using a fluorescent probe. https://doi.org/10.1016/0003-2697(89)90651-9

Kamo N, Muratsugu M, Hongoh R, Kobatake Y (1979) Membrane potential of mitochondria measured with an electrode sensitive to tetraphenyl phosphonium and relationship between proton electrochemical potential and phosphorylation potential in steady state. https://doi.org/10.1007/bf01868720

Kauppinen RA, Hassinen IE (1984) Monitoring of mitochondrial membrane potential in isolated perfused rat heart. https://doi.org/10.1152/ajpheart.1984.247.4.h508

Kiss G, Konrad C, Doczi J, Starkov AA, Kawamata H, Manfredi G, Zhang SF, Gibson GE, Beal MF, Adam-Vizi V, Chinopoulos C (2013) The negative impact of alpha-ketoglutarate dehydrogenase complex deficiency on matrix substrate-level phosphorylation. https://doi.org/10.1096/fj.12-220202

Komlódi T, Geibl FF, Sassani M, Ambrus A, Tretter L (2018) Membrane potential and delta pH dependency of reverse electron transport-associated hydrogen peroxide production in brain and heart mitochondria. https://doi.org/10.1007/s10863-018-9766-8

Korshunov SS, Skulachev VP, Starkov AA (1997) High protonic potential actuates a mechanism of production of reactive oxygen species in mitochondria. https://doi.org/10.1016/s0014-5793(97)01159-9

Krumschnabel G, Eigentler A, Fasching M, Gnaiger E (2014) Use of safranin for the assessment of mitochondrial membrane potential by high-resolution respirometry and fluorometry. https://doi.org/10.1016/b978-0-12-416618-9.00009-1

Lambeth DO, Tews KN, Adkins S, Frohlich D, Milavetz BI (2004) Expression of two succinyl-CoA synthetases with different nucleotide specificities in mammalian tissues. https://doi.org/10.1074/jbc.m406884200

Lambert AJ, Brand MD (2004) Superoxide production by NADH:ubiquinone oxidoreductase (complex I) depends on the pH gradient across the mitochondrial inner membrane. https://doi.org/10.1042/bj20040485

Ligeti E, Fonyo A (1977) Competitive inhibition of valinomycin-induced K+-transport by Mg2+-ions in liver mitochondria. https://doi.org/10.1016/0014-5793(77)80344-x

Metelkin E, Demin O, Kovács Z, Chinopoulos C (2009) Modeling of ATP-ADP steady-state exchange rate mediated by the adenine nucleotide translocase in isolated mitochondria. https://doi.org/10.1111/j.1742-4658.2009.07394.x

Mitchell P (1961) Coupling of phosphorylation to electron and hydrogen transfer by a chemi-osmotic type of mechanism. https://doi.org/10.1038/191144a0

Mitchell P (1967) Proton current flow in mitochondrial systems. https://doi.org/10.1038/2141327a0

Mitchell P, Moyle J (1968) Proton translocation coupled to ATP hydrolysis in rat liver mitochondria. https://doi.org/10.1111/j.1432-1033.1968.tb00245.x

Rieger B, Junge W, Busch KB (2014) Lateral pH gradient between OXPHOS complex IV and F(0)F(1) ATP-synthase in folded mitochondrial membranes. https://doi.org/10.1038/ncomms4103

Rieger B, Arroum T, Borowski MT, Villalta J, and Busch KB (2021) Mitochondrial F_1F_0 ATP synthase determines the local proton motive force at cristae rims. https://doi.org/10.15252/embr.202152727

Rolfe DF, Hulbert AJ, Brand MD (1994) Characteristics of mitochondrial proton leak and control of oxidative phosphorylation in the major oxygen-consuming tissues of the rat. https://doi.org/10.1016/0005-2728(94)90062-0.

Rosenthal RE, Hamud F, Fiskum G, Varghese PJ, Sharpe S (1987) Cerebral ischemia and reperfusion: prevention of brain mitochondrial injury by lidoflazine. https://doi.org/10.1038/jcbfm.1987.130

Rottenberg H (1984) Membrane potential and surface potential in mitochondria: uptake and binding of lipophilic cations. https://doi.org/10.1007/bf01868977

Rouslin W, Erickson JL, Solaro RJ (1986) Effects of oligomycin and acidosis on rates of ATP depletion in ischemic heart muscle. https://doi.org/10.1152/ajpheart.1986.250.3.h503

Scaduto Jr RC, Grotyohann LW (1999) Measurement of mitochondrial membrane potential using fluorescent rhodamine derivatives. https://doi.org/10.1016/s0006-3495(99)77214-0

Selivanov VA, Zeak JA, Roca J, Cascante M, Trucco M, Votyakova TV (2008) The role of external and matrix pH in mitochondrial reactive oxygen species generation. https://doi.org/10.1074/jbc.m801019200

Starkov AA, Fiskum G (2003) Regulation of brain mitochondrial H2O2 production by membrane potential and NAD(P)H redox state. https://doi.org/10.1046/j.1471-4159.2003.01908.x

Tretter L, Takacs K, Hegedüs V, Adam-Vizi V (2007) Characteristics of alpha-glycerophosphate-evoked H_2O_2 generation in brain mitochondria. https://doi.org/10.1111/j.1471-4159.2006.04223.x

Vajda S, Mándi M, Konràd C, Kiss G, Ambrus A, Adam-Vizi V, Chinopoulos C (2009) A re-evaluation of the role of matrix acidification in uncoupler-induced Ca^{2+} release from mitochondria. https://doi.org/10.1111/j.1742-4658.2009.06995.x

Votyakova TV, Reynolds IJ (2001) DeltaPsi(m)-Dependent and -independent production of reactive oxygen species by rat brain mitochondria. https://doi.org/10.1046/j.1471-4159.2001.00548.x

Walker JE (1994) The regulation of catalysis in ATP synthase. https://doi.org/10.1016/0959-440x(94)90274-7

Wolf DM, Segawa M, Kondadi AK, Anand R, Bailey ST, Reichert AS, van der Bliek AM, Shackelford DB, Liesa M, Shirihai OS (2019) Individual cristae within the same mitochondrion display different membrane potentials and are functionally independent. https://doi.org/10.15252/embj.2018101056

Zoccarato F, Miotto C, Cavallini L, Alexandre A (2011) The control of mitochondrial succinate-dependent H_2O_2 production. https://doi.org/10.1007/s10863-011-9363-6

Zółkiewska A, Czyz A, Duszyński J, Wojtczak L (1993) Continuous recording of intramitochondrial pH with fluorescent pH indicators: novel probes and limitations of the method. https://pubmed.ncbi.nlm.nih.gov/8212962